JOURNAL OF MATERIALS SCIENCE 21 (1986) 1161–1165

Anisotropic flow and fracture in beryl [$Be_3Al_2(SiO_3)_6$]

O. O. ADEWOYE
Department of Metallurgical and Materials Engineering, University of Ife, Ile-Ife, Oyo-State, Nigeria

Flow and fracture resulting from Vickers indentation testing on {0 0 0 1} and {1 0 $\bar{1}$ 0} planar orientations have been examined. Flow characterized by indent shape differentiation was analysed to belong to the slip system with planes of the types {1 0 $\bar{1}$ 0} and {1 1 $\bar{2}$ 0}. The ensuing fracture paths were resolved to propagate along {1 0 $\bar{1}$ 0} and {1 1 $\bar{2}$ 0} cleavage planes while K_c values obtained for them were 0.196 and 0.248 MPa m$^{1/2}$, respectively.

1. Introduction

In a recent publication [1], the anisotropy in the fracture of beryl indented on {1 0 $\bar{1}$ 0} plane was demonstrated despite the hitherto held belief that fracture in beryl is rather difficult [2] or imperfect (0 0 0 1) [3]. The present investigation extends the above quoted work [1] to the activation of fracture in orthogonal directions on the {0 0 0 1} surface and a further elucidation of cleavage on {1 0 $\bar{1}$ 0}. Plastic flow on both {0 0 0 1} and {1 0 $\bar{1}$ 0} planes are also examined. Load–radial crack plots are also made and values of the fracture toughness parameters K_c estimated.

2. Indentation fracture and mechanics

Indentation fracture has been demonstrated to be a useful and widely applicable field in the study of fracture behaviour of ceramic materials; while the theory of indentation fracture mechanics has been thoroughly elucidated in a number of publications [4–6]. It will suffice here to mention the forms of fracture and quote the relevant relationships that will be of use in the present analysis.

Fracture ensuing from the small tensile component of the applied stresses under the indenter and those associated with the residual stresses arising from the plastic constraint of the indentation area, have been shown to exist in two main modes. These are the lateral, which is parallel to the tested surface and, the more important for our analysis, the median/radial cracks. In a number of publications e.g. [5–7], it has been shown that while the elastic component drives the downward extension of the median cracks during the loading cycle, it is the residual component that provides the primary driving force during the unloading sequence when the median cracks forms its well-developed half-penny shape. In this analysis, the surface trace and dimension of the subsurface median crack are termed radial and C_R, respectively. A relationship between the applied central load P and C_R was obtained [6] as

$$K_c = \frac{P}{C_R^{3/2}} [\zeta_r^R (\cot \psi)^{2/3}] (E/H)^{1/2} \quad (1)$$

where C_R is the radial crack, ζ_r^R is a constant evaluated to be 0.032 $\pm$ 0.002 [6, 7], ψ, the indenter cone half angle, K_c is critical stress intensity factor and (E/H) is the ratio of Young's modulus to the hardness which must be known for each material.

In crystalline solids however, orthogonal radial/median cracks can be induced to form on planes of easy cleavage rather than to exist as high energy-requiring conchoidal fracture. For hexagonal crystals, this would mean the preferential alignment of the indenter axes on the {0 0 0 1} plane, along ⟨1 0 $\bar{1}$ 0⟩ and ⟨1 $\bar{2}$ 1 0⟩ and; on the {1 0 $\bar{1}$ 0} plane, along the ⟨1 $\bar{2}$ 1 0⟩ and ⟨0 0 0 1⟩ for those specific structures whose cleavage planes are of the types {1 $\bar{2}$ 1 0}, {1 0 $\bar{1}$ 0} and {0 0 0 1}. Examples of such are SiC [8] and Al_2O_3 [7]. This has been done in this case and is reported in Section 4.

3. Experimental details

Naturally occurring samples of beryl from Ife and Lokoja in Nigeria were utilized in the experiments. X-ray diffractometer runs were carried out and the values of the c/a ratio obtained showed no difference from the one already reported for beryl from Ife [1]. Both the {0 0 0 1} and {1 0 $\bar{1}$ 0} faces of as-grown samples were tested, after etching in 60% HF to reveal fresh (as opposed to already deformed) areas on a Beuhler Micromet Microhardness tester fitted with a Vicker Diamond Indenter. The axes of the indenter were aligned at specific orientations as follows: on the {0 0 0 1} plane, the axes were aligned along the ⟨1 0 $\bar{1}$ 0⟩ and the ⟨1 1 $\bar{2}$ 0⟩; on the {1 0 $\bar{1}$ 0} plane, the axes were aligned along the ⟨0 0 0 1⟩ and ⟨1 $\bar{2}$ 1 0⟩*. In this way, propagating median and radial cracks can lie along orthogonal cleavage planes. Micrographs depicting

*For the sake of convenience, directions in the hexagonal system will be referred to as indicated in Fig. 1; while directions on individual micrographs will also be appropriately labelled.

0022–2461/86 $03.00 + .12

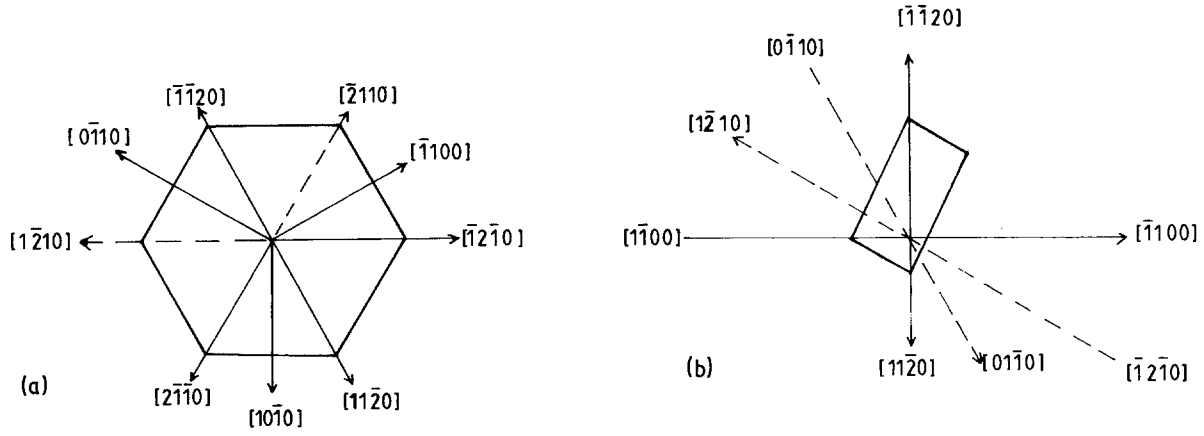

Figure 1 Schematic diagram showing (a) principal directions in the ⟨0 0 0 1⟩ zone of the hexagonal system and (b) an associated diagram of these principal directions in relation to the facets of the indenter as delianated by the sides of the indent (Fig. 1b is also a schematic of Fig. 2b).

flow and fracture were taken and they are shown in Figs. 2a to f. Values of C_R, half the width of radial cracks were measured as a function of increasing load and used in Equation 1 to estimate values of K_c. A plot of P_c against $C_R^{3/2}$ is given in Fig. 3 and the values of K_c, measured are also given in Table I.

4. Results and discussion

4.1. Plastic flow

Plastic flow, resulting from the operation of slip-systems in the subsurface region beneath the Vickers indenter, affects the shape of the ensuing indentation in such a way as to reflect the crystallography of the slip-system. The shape of the indent is therefore diagnostic and especially useful in the determination of the properties of ceramic materials where the conventional ambient temperature tensile testing for the determination of plastic flow is not possible. The shape of the Vickers indentation, which is mainly cubic in an isotropic medium following the four-fold symmetry of the indenter will at least be distorted or in fact change its geometry when modulated by the crystallography of flow of the underlying material. This has been aptly demonstrated [9–11]. This shape will remain substantially cubic in faces of four-fold symmetries and often with modifications, reflecting flow as explained above, e.g. leading to either pin-cushioning or barelling [11]. In hexagonal materials, the shape may vary from asymmetrically-distorted cubic (e.g. on (0 0 0 1) of SiC [12]), to rectangular with or without distortion along one of the principal axes on the {0 0 0 1} (e.g. Figs. 2b and c), or pin-cushioning or barelling along the principal axes on {1 0 $\bar{1}$ 0} [1].

In general, this diagnostic shape change is more amenable to interpretation in cases where there is coincidence between the symmetries of the test plane and the four-fold symmetry of the indenter. There in essence lies the relative ease with which changes in shape of indentations in a cubic system is understood more readily than those occurring in hexagonal systems. Hence, more work concerning indentation induced flow have been reported for cubic systems [9–11]. Dislocation reactions, arising from indentation testing and leading to flow in hexagonal crystals have however, not received much attention. This is not to say that dislocation reactions in hexagonal crystals in general have not been studied in detail. Notable in this regard are the works of Heuer *et al.* on alumina [13].

This however, is not to say that information pertaining to flow from indentation testing is not available within the vicinity of the indent in hexagonal materials. For instance, the slightly asymmetric Vickers indentation on SiC when etched revealed on the same site, a pit with hexagonal symmetry which is consistent with flow on the {0 h $\bar{h}$ l} plane in the ⟨2 $\bar{1}$ $\bar{1}$ 0⟩ direction [14].

In the present work, even though the details of the slip system controlling the shape of the indentations have not been worked out, nevertheless, information pertinent to such an understanding can be deduced from the indents as follows. Differential flow in beryl was noticed from changes in shapes of indents on both the {0 0 0 1} and the {1 0 $\bar{1}$ 0} for each of the two orientations (i.e. ⟨2 $\bar{1}$ $\bar{1}$ 0⟩ and ⟨1 0 $\bar{1}$ 0⟩ on {0 0 0 1} and, ⟨0 0 0 1⟩ and ⟨1 $\bar{2}$ 1 0⟩ on the {1 0 $\bar{1}$ 0}). For the {0 0 0 1} plane, two types of shape changes were noticed. One, consistent with sinking-in occurs for indents aligned along both the ⟨1 $\bar{2}$ 1 0⟩ and ⟨1 0 $\bar{1}$ 0⟩. These are shown in Figs. 2a and c. A second type, noticed for some ⟨1 $\bar{2}$ 1 0⟩ indentations, is consistent with a shape change from cubic to rectangular. An example of this is shown in Fig. 2b. The first type, easier to conceptualize as material differentiation, arising from sinking-in, is due to plastic flow, even though the details of the atomic mobilities leading to such flow are yet to be elucidated. A second type, is elongated along sides whose normal bisects the 30° angle subtended by the directions [1 $\bar{2}$ 1 0]–[$\bar{1}$ 2 $\bar{1}$ 0] and [0 $\bar{1}$ 1 0]–[0 1 $\bar{1}$ 0], and also foreshortened along its other sides whose normal bisects the angle subtended by the directions [$\bar{2}$ 1 1 0]–[2 $\bar{1}$ $\bar{1}$ 0] and [$\bar{1}$ 0 1 0]–[1 0 $\bar{1}$ 0].

TABLE I Orientation dependence of critical stress intensity factor K_c in beryl

Orientation				
Plane	Direction	E(GPa)	H(GPa)	K_c(MPa m$^{1/2}$)
{0 0 0 1}	⟨2 $\bar{1}$ $\bar{1}$ 0⟩	219	12.07	0.196
{0 0 0 1}	⟨1 0 $\bar{1}$ 0⟩	219	12.29	0.248

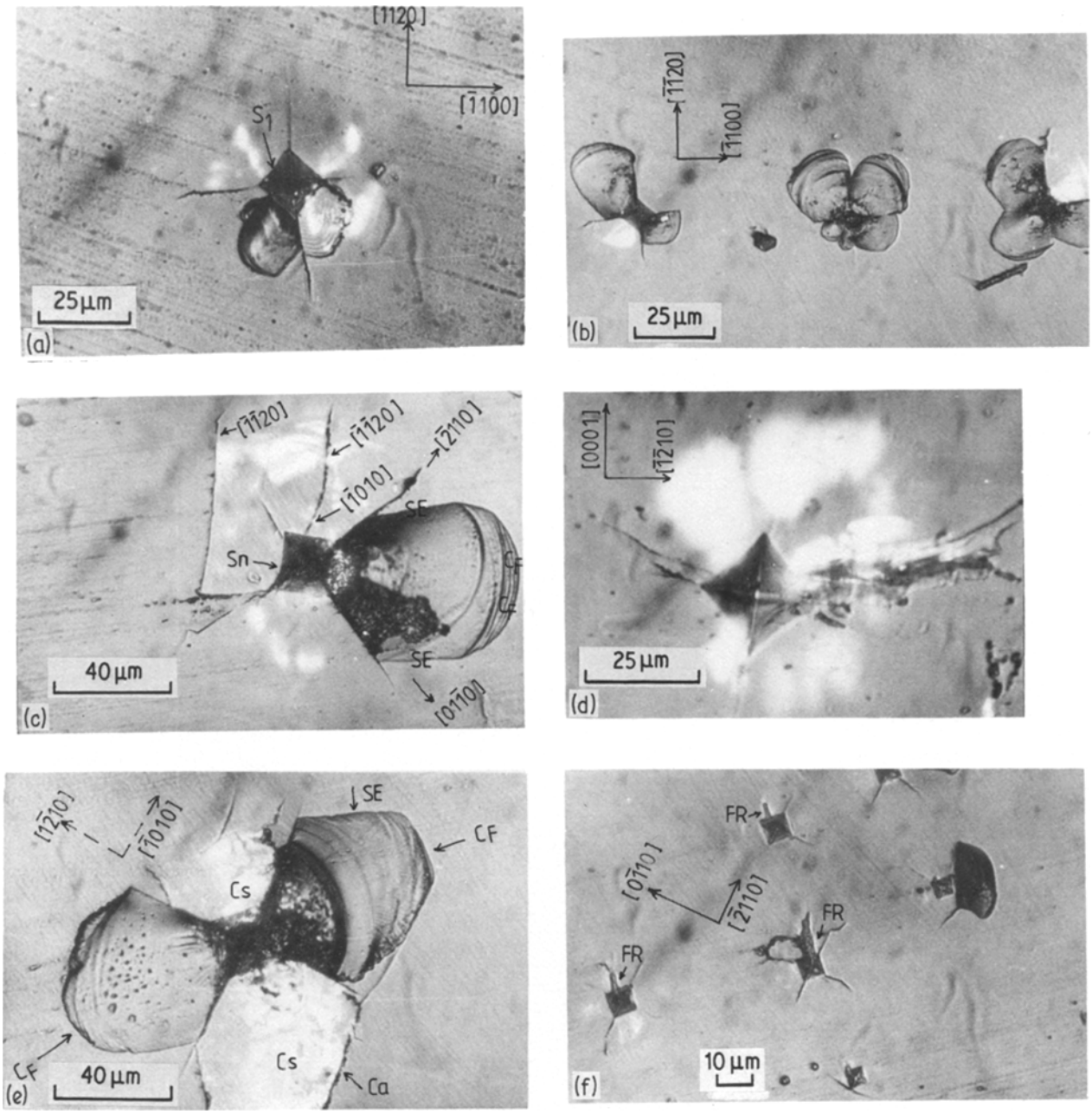

Figure 2 Optical micrographs of flow and fracture in beryl resulting from Vickers indentation in the load range 0.025 to 0.5 N. (a) An indent made along the $[\bar{1}\,\bar{1}\,2\,0]$–$[1\,1\,\bar{2}\,0]$ direction at a load of 0.3 N. The sinking-in on one side of the indent denoting irreversible plastic flow is to be noticed at S_1. This is compared to micrograph Fig. 2c for indent along the $[0\,\bar{1}\,1\,0]$. (b) A rectangular shape of the indent on the $\{0\,0\,0\,1\}$ face of beryl tested along the $[\bar{1}\,\bar{1}\,2\,0]$–$[1\,1\,\bar{2}\,0]$ (see Section 4.2, load = 0.3 N). (c) The micrograph shows an indent along the $[0\,\bar{1}\,1\,0]$ direction on the $\{0\,0\,0\,1\}$ plane. Sinking-in of an elongated (into rectangular shape) indent is seen at Sn. In addition to fracture along the tested $[0\,\bar{1}\,1\,0]$ and the requisite $[\bar{2}\,1\,1\,0]$ at $\pi/2$ to it, fracture also occurs along directions $[\bar{1}\,\bar{1}\,2\,0]$ away from the indent and also, along the $[\bar{1}\,0\,1\,0]$ which later changes to the $[\bar{1}\,\bar{1}\,2\,0]$. Lateral cracking, with evidence of progressive layering, in a conchoidal manner is seen at CF while straight edges of the same vent denoting trace of a cleavage plane is observed at SE (load = 0.5 N). (d) Sinking-in on $\{1\,0\,\bar{1}\,0\}$ with indenter axes aligned along $\langle 0\,0\,0\,1\rangle$. The same shape is also observed, when the indenter is aligned along $\langle 1\,1\,\bar{2}\,0\rangle$, the cracks here, typical of most of the cracks observed on the $\{1\,0\,\bar{1}\,0\}$ plane do not propagate, usually along known cleavage planes in contrast to those observed for cracks on $\{0\,0\,0\,1\}$ (e.g. Fig. 2e). (e) An indent along $[1\,\bar{2}\,1\,0]$ exhibiting cleavage along both $[1\,\bar{2}\,1\,0]$–$[\bar{1}\,2\,\bar{1}\,0]$ and $[\bar{1}\,0\,1\,0]$–$[1\,0\,\bar{1}\,0]$ directions. The symmetrical nature of the fracture modes associated with indent is to be noted, CF and SE are as already explained above (Fig. 2d). Cleavage along the $[1\,0\,\bar{1}\,0]$ away from the indent is to be noted at Ca. (f) Rectangular fracture feature at low loads on the $\{0\,0\,0\,1\}$ surface along the $[0\,\bar{1}\,1\,0]$ direction is to be noted at FR (see Section 4.2.).

This latter shape change may also be due to plastic flow although such flow is more difficult to explain when compared to the sinking-in. Alternatively, this could be due to the presence of lateral cracks causing a displacement whereby the equilibrium configuration post-indentation is rectangular and not cubical. Elongation in addition to sinking-in on one side is also observed (Fig. 2c). Similarly, for tests conducted on the $\{1\,0\,\bar{1}\,0\}$, sinking-in is observed for both orientations in directions denoting flow along orthogonal $\langle 0\,0\,0\,1\rangle$ and $\langle 2\,\bar{1}\,\bar{1}\,0\rangle$ directions (Fig. 2d). Changes in shape or sinking-in as observed in Figs. 2a to d unfortunately do not define for us unambiguously the slip systems controlling flow. In Fig. 2c for instance, the indenter is aligned along the $[0\,\bar{1}\,1\,0]$ direction with the median cracks aligned along $[0\,\bar{1}\,1\,0]$–$[0\,1\,\bar{1}\,0]$ and $[2\,\bar{1}\,\bar{1}\,0]$–$[\bar{2}\,1\,1\,0]$ directions. The sinking-in of the indent is contributed to by the $[1\,\bar{2}\,1\,0]$ and $[1\,\bar{1}\,0\,0]$ directions,

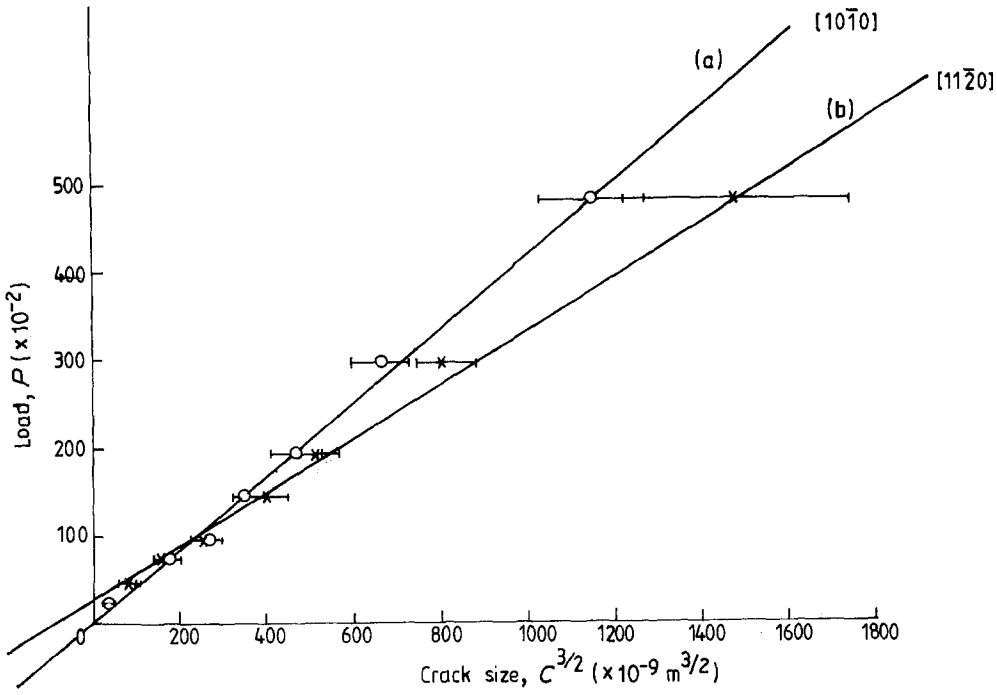

Figure 3 Applied load P against crack parameter $C^{3/2}$ on the $\{0\,0\,0\,1\}$ plane of beryl. (a) and (b) denote results for measurements along the $\langle 1\,1\,\bar{2}\,0\rangle$ and $\langle 1\,0\,\bar{1}\,0\rangle$ axes, respectively.

in which case the flow plane(s) responsible for the sinking-in could have been any for which these two directions are zone axes. These suggest a plane of the type $\{h\,0\,\bar{h}\,l\}$. However, judging from the fact that fracture planes of easy cleavage have been identified as $\{1\,0\,\bar{1}\,0\}$ and $\{2\,\bar{1}\,\bar{1}\,0\}$ (see Section 4.2) respectively, and given that in many hexagonal ceramic systems, there exists a coincidence of flow and fracture plane, (e.g. [15]), flow planes can be tentatively assigned to the type $\{1\,0\,\bar{1}\,0\}$ and $\{1\,1\,\bar{2}\,0\}$ types.

4.2. Morphology and crystallography of fracture

In general, crystallographic, conchoidal and subsurface cracking occur in beryl on both the $\{0\,0\,0\,1\}$ and the $\{1\,0\,\bar{1}\,0\}$ tested surfaces with a predominance of cleavage. The incidence, morphology and crystallography, all depend on a normally applied load, surface and angular orientation.

Cracking in all the four orientations on the two surfaces occurred at all loads from 0.025 to 0.5 N except for the 0° orientation on the $\{0\,0\,0\,1\}$ (i.e. $\langle 2\,\bar{1}\,\bar{1}\,0\rangle$) where cracking did not occur until 0.05 N.

For the $\{0\,0\,0\,1\}$, tested along $\langle 2\,\bar{1}\,\bar{1}\,0\rangle$, crystallographic cracking appeared both the $\langle 2\,\bar{1}\,\bar{1}\,0\rangle$ tested direction and the requisite $\langle 1\,0\,\bar{1}\,0\rangle$ at 90° to the test direction; these being along the axes of the indenter (e.g. Fig. 2e). The existence of crystallographic cleavage along the $\langle 1\,\bar{2}\,1\,0\rangle$ and $\langle 1\,0\,\bar{1}\,0\rangle$ axes on the $\{0\,0\,0\,1\}$ plane also occurred for tests conducted along the $\{1\,0\,\bar{1}\,0\}$ (Fig. 2c). Lateral cracking, with cleavage facets parallel to $\{0\,0\,0\,1\}$, and often bounded by both conchoidal cracks and at least in some part by straight edges, hence crystallographic in nature, and thus denoting the activation of cleavage planes quite distinct from those emanating from the ends of the indentations exist (see C_F, C_E in Fig. 2c and e, respectively).

A crystallographic fracture, (observed and shown in Fig. 2f) features, are noticeable for 30° indents and sporadic for indents at 60°, but not at all for 0° indents which occur at loads below 0.15 N for indents on the $\{0\,0\,0\,1\}$. The projections of these fracture surfaces are bounded by lines parallel and perpendicular to the sides of the indents.

Their rectangular nature, denoting orientation dependence suggest cleavage rather than conchoidal fracture. Their planar orientation are however not clear as of now. The fact that their rectangular edges are at angle 45° to indenter axes, an angle not between principal directions, however suggests these features belong to cleavage of higher index planes rather than simple indexed ones.

Except for a few cases (e.g. Figs. 2c and d of reference [1]) fracture paths for indentations on the $\{1\,0\,\bar{1}\,0\}$ plane made along both the $\langle 0\,0\,0\,1\rangle$ and $\langle 2\,\bar{1}\,\bar{1}\,0\rangle$ occur along directions other than those of the principal axes of the indenter. In a few cases where such paths occurred along the $\langle 0\,0\,0\,1\rangle$ and $\langle 1\,1\,\bar{2}\,0\rangle$, hence denoting cleavage of planes for which those directions are zone axes, they did so along with the other, more numerous type. This sort of non-occurrence of fracture paths along the principal axis has also been observed on Al_2O_3-$(0\,0\,0\,1)$ [7], and SiC-$(0\,0\,0\,1)$ [8] and has been previously reported for indentation on beryl – $\{1\,0\,\bar{1}\,0\}$ along the $\langle 0\,0\,0\,1\rangle$ [1].

Given that fracture on the $\{0\,0\,0\,1\}$ occurs predominantly along the $\langle 2\,\bar{1}\,\bar{1}\,0\rangle$ and $\langle 1\,\bar{1}\,0\,0\rangle$ and that on the $\{1\,0\,\bar{1}\,0\}$ it has occurred along the $\langle 1\,1\,\bar{2}\,0\rangle$ and $\langle 0\,0\,0\,1\rangle$, both the $\{1\,0\,\bar{1}\,0\}$, and $\{1\,1\,\bar{2}\,0\}$ cleavage planes do occur in beryl.

The relation in Equation 1 was plotted and a least square fit analysis of results undertaken. As it can be observed in Fig. 3, a linear plot was obtained for P against $C^{3/2}$ thus confirming the applicability of the

relation for beryl in the estimation of K_C for single crystals. This relation has also been found to be true for cleavage in Al_2O_3 [7] and SiC [8].

The variable H in the ratio (E/H) in Equation 1 was obtained by taking the averages of Vickers indentation diagonals (d) and using the relation

$$H = \frac{P}{2\alpha^2}$$

where $\alpha = \frac{1}{2}d$, while E, the Young's modulus was obtained from the open literature [16]. Values of 0.196 and 0.248 MPa $m^{1/2}$ were obtained for $\{1\,0\,\bar{1}\,0\}$ and $\{1\,1\,\bar{2}\,0\}$ cleavage planes.

Conclusion

In conclusion, extensive anisotropic flow and fracture occur in beryl. Even though unambiguous and explicit determination of the slip planes have not been made, evidence available from the pin-cushioning effect of indentations on both the $\{0\,0\,0\,1\}$ and the $\{1\,0\,\bar{1}\,0\}$ tested surfaces suggest that there is a coincidence between the fracture and flow planes. In other words, these planes belong to the $\{1\,0\,\bar{1}\,0\}$ and $\{1\,\bar{2}\,1\,0\}$ families. Therefore, the most likely flow and fracture planes have been determined as belonging to the $\{1\,0\,\bar{1}\,0\}$ and $\{1\,1\,\bar{2}\,0\}$ families. In contrast to the belief in the literature (e.g. [2, 3]), this work has demonstrated that fracture in beryl is not just conchoidal, but anisotropic as well. Furthermore, K_C for $\{1\,0\,\bar{1}\,0\}$ and $\{1\,1\,\bar{2}\,0\}$ planes have been determined as 0.196 and 0.248 MPa $m^{1/2}$, respectively.

Acknowledgement

The author gratefully acknowledges the University of Ife for research support through research grant no. 14.25 EW.

References

1. O. O. ADEWOYE, *J. Mater. Sci. Lett.* **3** (1984) 855.
2. A. N. WINCHELL, in "Elements of Optical Mineralogy part III, Determinative Tables" 2nd Edn. (John Wiley, London, 1962) pp. 30–1.
3. R. WEBSTER, in "GEMS" 3rd edn. (Archon Books, Hamden, Connecticut, 1975) p. 563.
4. B. R. LAWN and T. R. WILSHAW, *J. Mater. Sci.* **10** (1975) 1049.
5. B. R. LAWN, in "Fracture Mechanics of Ceramics" edited by R. C. Bradt, A. G. Evans, D. P. H. Hasselman and F. F. Large (Plenum Press, New York 1983) Vol. 5, pp. 1–26.
6. B. R. LAWN, A. G. EVANS and D. B. MARSHALL, *J. Amer. Ceram. Soc.* **63** (1980) 574.
7. S. S. SMITH and B. J. PLEKTA, in "Fracture Mechanics of Ceramics" edited by R. C. Bradt, A. G. Evans, D. P. H. Hasselman and F. F. Large (Plenum Press, New York, 1983) Vol. 5, p. 189.
8. O. O. ADEWOYE, *ibid.* p. 107.
9. A. S. KEH, *J. Appl. Phys.* **31** (1960) 1358.
10. J. J. GILMAN, *ibid.* **44** (1973) 982.
11. R. W. ARMSTRONG and C. C. WU, *J. Amer. Ceram. Soc.* **61** (1978) 102.
12. O. O. ADEWOYE, PhD thesis University of Cambridge, Cambridge (1976).
13. B. J. PLEKTA, T. E. MITCHELL and A. H. HEUER, *J. Amer. Ceram. Soc.* **57** (1979) 388.
14. O. O. ADEWOYE and T. F. PAGE, *J. Mater. Sci.* **11** (1976) 981.
15. F. R. N. NABBARO, in "Theory of Crystal Dislocations" (Clarendon Press, Oxford, 1967) p. 239.
16. F. BIRCH, *Amer. Mineralogist* **35** (1955) 649.

Received 21 December 1984
and accepted 13 May 1985